



## Research article

# Design optimization and validation of UV-C illumination chamber for filtering facepiece respirators

Abu S.M. Mohsin<sup>a,\*</sup>, Mohd. Raed Jamiruddin<sup>b,c,\*\*</sup>, Md Mahmudul Kabir Peyal<sup>a</sup>, Shahana Sharmin<sup>b</sup>, Ashfaq Ahmed<sup>b</sup>, Afrin Hossain Puspita<sup>a</sup>, A.A.M. Sharfuddin<sup>b</sup>, Afrida Malik<sup>a</sup>, Al Hasib<sup>b</sup>, Sanjida Akter Suchona<sup>b</sup>, Arshad M. Chowdhury<sup>a</sup>, Eva Rahman Kabir<sup>b</sup>

<sup>a</sup> Department of Electrical and Electronics Engineering, Brac University, 66 Mohakhali, Dhaka, Bangladesh

<sup>b</sup> School of Pharmacy, Brac University, 66 Mohakhali, Dhaka, Bangladesh

<sup>c</sup> Gonoshasthaya-RNA Molecular Diagnostic and Research Center, Dhaka, Bangladesh

## ARTICLE INFO

## Keywords:

UV-C illumination chamber  
SAR-CoV-2 virus  
Facepiece respirators  
Personal protection equipment (PPE)  
Decontamination efficacy  
Biological decontamination and pathogens

## ABSTRACT

In this study, we constructed an UV-C illumination chamber using commercially available germicidal lamps and other locally available low-cost components for general-purpose biological decontamination purposes. The illumination chamber provides uniform illumination of around 1 J/cm<sup>2</sup> in under 5 min across the chamber. The control mechanism was developed to automate the on/off process and make it more secure minimizing health and other electrical safety. To validate the decontamination efficacy of the UV-C Illumination Chamber we performed the *Geobacillus* spore strip culture assay. Additionally, we performed the viral load measurement by identifying the COVID-19-specific N-gene and ORF1 gene on surgical masks. The gold standard RT-qPCR measurement was performed to detect and quantify the COVID-19-specific gene on the mask sample. The biochemical assay was conducted on the control and test group to identify the presence of different types of bacteria, and fungi before and after exposure under the illumination chamber. The findings of our study revealed satisfactory decontamination efficacy test results. Therefore, it could be an excellent device in healthcare settings as a disinfection tool for biological decontamination such as SAR-CoV-2 virus, personal protection equipment (PPE), (including n95, k95 respirators, and surgical masks), and other common pathogens.

## 1. Introduction

The recent global pandemic of COVID-19 has created a high demand for personal protection equipment (PPE) including facepiece respirators such as N95, K95 or surgical masks etc. Unfortunately, the current supply cannot satisfy the growing high demand.

Several state of art decontamination methods have been reported in literature which discuss various methods for decontaminating N95 respirators for reuse during the COVID-19 pandemic. The reported decontamination methods are ultraviolet germicidal irradiation (UVGI), hydrogen peroxide vaporization (VHP), microwave-generated steaming, autoclave treatment, ethylene oxide gassing

\* Corresponding author.

\*\* Corresponding author. School of Pharmacy, Brac University, 66 Mohakhali, Dhaka, Bangladesh.

E-mail addresses: [asm.mohsin@bracu.ac.bd](mailto:asm.mohsin@bracu.ac.bd) (A.S.M. Mohsin), [mohd.raeed@bracu.ac.bd](mailto:mohd.raeed@bracu.ac.bd) (Mohd.R. Jamiruddin).

(ETO), low temperature hydrogen peroxide gas plasma (LT-HPGP) treatment, peracetic acid dry fogging (PAF), moist heat (MH) treatment and dry heating [1–4]. In a recent study, researchers discussed vaporized hydrogen peroxide (VHP), ultraviolet light (UV), and ethanol and found VHP treatment most effective, with no significant change after two treatments, while ethanol and UV decontamination showed functional degradation to different degrees [1]. As per their findings the VHP method can effectively disinfect N95 masks contaminated with SARS-CoV-2 and ESKAPE bacteria [1].

Given successful inactivation of SARS-CoV-2 combined with maintained functional integrity following 5 cycles of decontamination, peracetic acid dry fogging, VHP, autoclaving (for a subset of masks), and moist heat treatment are viable options for decontamination of most models of N95 masks [4].

In another study Limei et al. [5] developed the protective equipment fumigation sterilization cabinet and achieves the complete sterilization of the PPRPHs when the air flow is at 10.5–12.3 m<sup>3</sup>/h. A medical mask with a plasma layer [6] provides both additional air filtration from micro drops, bacteria, and viruses due to the electrostatic effect and self-disinfecting of surfaces by a pulsed barrier discharge. Steam sterilization [7] of N95 masks is effective for reducing infection in clinicians. The pulsed-xenon ultraviolet room disinfection [8] showed a statistically significant reduction in microbial load and eliminated vancomycin-resistant enterococci on sampled surfaces when using a 12-min multilocation treatment cycle. A hydrogen peroxides [9] dry fumigation system seemed to have a good sporicidal effect when used in rooms, ambulances, and external and internal parts of ventilated equipment. The immersion in 80 °C water and the microwave-assisted sterilization [10] achieved a high degree of mask decontamination without altering the filtration efficiency and breathability. Vaporized hydrogen peroxide mask disinfection systems [11] are being deployed at multiple locations throughout the United States.

In another study ultraviolet germicidal irradiation (UVGI), commonly known as UV-C was reported as effective decontamination methods for air, water, and surface decontamination [3]. The wavelength of UV-C is around 200 nm–280 nm. It has been reported in several studies that UVGI exposure can inactivate pathogens by damaging the nucleic acid genome inhibiting replication process [3]. Based on the available evidence, the recommended cumulative dose for clinical application of UVGI and/or further investigation is no less than 20,000 and ideally 40,000 J/m<sup>2</sup>. A cumulative dose above 20,000 J/m<sup>2</sup> resulted in a 2-log reduction in viral load, while a dose above 40,000 J/m<sup>2</sup> consistently resulted in a 3-log reduction in viral pathogens [2]. In a recent study dosage of 1 J/cm<sup>2</sup> (fluence level) has been shown to be effective for inactivating growth of numerous viruses and bacteria [3].

On the other hand a discernible increase in the usage and manufacture of face masks has been reported worldwide since the COVID-19 pandemic emerged. The global market for disposable masks has expanded from \$0.73 billion to \$22 billion annually due to governments mandating the wearing of face masks in public places [12–15]. The enormous use of face masks has drawn attention recently due to waste generation, which endangers the environment as it is used a million times each day globally and requires more energy and raw materials to manufacture [13,16–18]. Moreover, these used masks are discarded in public spaces which impacts the environment and threatens the ecosystem due to improper and mismanaged disposal [19,20]. Following soil exposure, the ecotoxicological impacts of these wastes on immunologic parameters, survival, reproduction, and energy-related parameters were investigated [12,14,21–23].

Furthermore, health experts warn that improperly discarded masks can spread viral diseases throughout a community [19,24,25]. Face mask disposal is an uppermost concern in the post-pandemic stage. Recent waste disposal techniques include burning and landfilling, which are inappropriate public health solutions. Some other prevention methods are heating sterilization, filtering, chemical disinfectant agents, and ultraviolet irradiation, which might reduce the risk of viral infection. UV-C technology is used to reuse masks after disinfection, which might reduce pollution and save money worldwide [12,26–28].

Not only proper disposal but also the shortage of available personal protective equipment (PPE) poses concerns to tackle respiratory transmissible pandemics. During the COVID-19 pandemic, there has been a global shortage of face masks as both healthcare workers and patients were instructed to use them on a regular basis [29]. As of 1 August 2021, nearly 2.5 million masks were sold per day in Bangladesh [30]. To cope with the high demand for surgical face masks, it will be an expensive approach to go for manufacturing on such a high scale [31]. One effective measure could be the reusability of face masks.

To combat supply shortage of PPEs, face masks and proper disposing mechanisms, we designed a cost effective and efficient UV-C disinfecting chamber. The development of our UV-Chamber explicitly proposes the re-utilization of personal protective equipment, thereby mitigating the degree of hazard faced by their scarcity.

## 2. Background study

In literature several studies have been conducted to identify the proper exposure wavelength and fluence level for decontamination purposes. Niels Finsen received the Nobel Prize in 1903 for discovering the importance of ultraviolet (UV) light in destroying germs [32]. As a result, it has been an effective technique, notably used by hospitals for several years, in disinfecting surgical suites to reduce the spread of medication-resistant pathogens. The exposure of UVGI (UV-germicidal irradiation), also known as UV-C inactivates pathogens by damaging their nucleic acid genomic material thus inhibiting their replication processes. It has been proven that at exposure levels of 1 J/cm<sup>2</sup> UV-C has effectively inactivated the growth of numerous viruses and bacteria [33]. With an energy spectrum from 3 eV to 6 eV and 200–280 nm wavelengths C-band, UV radiation can shed the outer-protein structure of the SARS-CoV-2, the coronavirus that causes COVID-19, thereby effectively killing the virus. The first 99.9% sterilization of SARS-CoV-2 was demonstrated by a company named Seoul Viosys using ultraviolet LEDs [34]. They do so by positioning their Violed LED modules at 3 cm distance and emit doses with 30 s intervals, however, the distance of 3 cm renders it ineffective to be used in large spaces. This further strengthens the potential effectiveness of the chamber in disinfecting the masks, as it shows that UV light can in fact be used in tight spaces to diminish the virus to a greater extent. L. R. Dougall [35] in his paper, explores the use and efficiency of pulsed ultraviolet

light decontamination of artificially generated microbiological aerosols and shows significant operational advantages over continuous UV light decontamination. It is imperative to ensure that the design of the disinfecting chamber is optimum and cost-effective. The paper also highlights the importance of maintaining safety regulations and implementing this light-based technology in sealed rooms. Another paper by Purshke et al. [3], provides an in-detail overview of the construction of three types of disinfection chamber using optical ray trace model that can be quickly deployed using commonly available components and subsystems, in order to enable a “safe” and “effective large-scale decontamination” of N95 masks [3]. The paper examines the use of three different optimal designs, the horizontal cabinet, the vertical cabinet, and the cylindrical design. The paper stresses the importance of uniform irradiance over 2 square meters, with a fluency level of  $1 \text{ J/cm}^2$  in 5 min, on the front, back and curved side surfaces of the N95 filter mask. As stated in the paper, this level of dosage would achieve a “minimum, a 3-log reduction of SARS-CoV-2 analogues (i.e., 99.9% inactivation), per FDA guidelines for N95 Tier 3 bioburden reduction” [3]. Furthermore, the paper prioritizes the need for a high throughput to counter the ever-increasing number of cases. Thomas M. Baer [3] proposes a design that was completed in two days by a single person using standard hand tools. Such a design can enable the disinfection of a large number of masks on a daily basis. Scott Mechler [36] elaborates on the use of different types of masks and respirators and how to properly clean them. When it came to using UVGI for N95, he stated that both dosage and wavelength of UV light are critical for inactivation of the virus. Therefore, it is crucial while designing a disinfecting procedure to remember that any part of the mask in shadow will not be disinfected. This could be a problem since penetrating the inner layers of certain mask designs could be difficult. He also says how, “Certain strap designs prone to twisting may also inhibit UVGI disinfection and a secondary disinfection step only applied to the straps of the mask may be necessary to counteract this.” Author Lindsay Kalter [37] mentions the increasing popularity of UV due to its disinfecting properties which made it commercially available, but also fairly warns on the “permanent damage” this light can cause and advises to use it with caution. In addition, Jeffrey P. Wilde et al. shows in their paper “Modeling UV-C irradiation chambers for mask decontamination using Zemax OpticStudio” the application of Zemax OpticStudio for modeling rectangular and cylindrical can shape UV-C decontamination chamber [38]. They have also proved from their result that rectangular and cylindrical geometrical cabinets can decontaminate N95 mask array by measuring illumination times with irradiance which can reach the accurate decontamination exposure level of  $1 \text{ J/cm}^2$ .

While designing the chamber, the crucial factors to consider are its effectiveness both in terms of design and cost of production while ensuring the safety in reusability. In addition, an optimum design must be used such that a UV-ray target to the mask from multiple angles can disinfect quickly and efficiently.

The main design inspiration behind this chamber is from the acclaimed Stanford University, USA [3] but it has been modified in a way to be portable and cost-effective with advanced control mechanisms which would make it feasible for most hospitals to access it.

### 3. Methodology

#### 3.1. Construction of chamber

The constructed Chamber was 180 cm tall by 90 cm wide by 60 cm deep (Fig. 1). A total of sixteen UV-C lights of 30 W would be fixed in the chamber with a gap of 23 cm between each. The UV-C has appeared to be effective in inactivating the growth of countless viruses and bacteria when exposed to levels of  $1 \text{ J/cm}^2$ . The uniform UV-C illumination exposes approximately two square meters. The illumination is adequate over this area to reach the generally accepted decontamination fluency level of  $1 \text{ J/cm}^2$  in less than 5 min. The



**Fig. 1.** Final prototype of UVC disinfection chamber. The image left without illumination (a) and right after illumination (b) shows the UV-C chamber.

wavelength of UV-C light is between 200 nm and 280 nm. The empty interior chamber gives a constant intensity variation of only 10%. The UVC intensity is around  $6.0\text{mw}/\text{cm}^2$  at the center of the chamber. The constant intensity would be exposed on the mask surfaces with different angles to interact with mask curvature. Initial measurement shows about 10%–15% of light has been transmitted through the mask. It is estimated that 5 min is adequate to allow  $1\text{ J}/\text{cm}^2$  to disinfect masks or biological samples.

The aluminum foil would be used to reflect the maximum amount of light of UV-C. The shiny side of the foil would be facing a cabinet wall. For the range of mentioned wavelengths, Aluminum could be an effective reflector of approximately 80%. The thermal energy produced during this operation would also be limited. The maximum temperature of the cabinet could reach up to  $40^\circ$  and humidity up to 20% with an intensity of 160 arbitrary units (a.u). Hence operations for long hours could not bring the temperature to the thresholds which could damage the mask.

Around 500 W of power is required to glow all the UV- C Lights. In the chamber, the intensity of UV-C would be about 50% of the total intensity evaluated by the detector or an average level of about  $6\text{ mW}/\text{cm}^2$ . The masks are contoured in 3 dimensions assuming 80% absorption of the incident light. The transmitted light is assumed to be scattered by the mask. The intensity in the chamber reduced to  $6\text{mw}/\text{cm}^2$  indicating a cutting of 25%. If we place 30 to 40 masks in rows, 5 masks adjusting in each row of the UV-C chamber, then 24-h operation assuming each batch requires 5 min per operation, could give an output of 5000 to 8000 masks per day.

Since the chamber is made of stainless steel it is imperative to take accurate safety measures to prevent short circuits and electrocution which could result in fatal incidents. The device is grounded and transmits a current of around 1.5–2 A. A fuse of 5 A is used as a precaution as well as an MCB (miniature circuit breaker) of 6 A is used around the UV lamps to prevent overload and short circuit.

In order to protect the cables from any faulty insulation, a BRB (Fire Protective) cable casing was used along with aluminum and paper on each side to prevent current flow on both sides. Glass Fiber coated wire commonly known as mica was used to further prevent spreading of any fire in case of a short circuit or spark. The entire wire system has been covered in a plastic box for added insulation. A

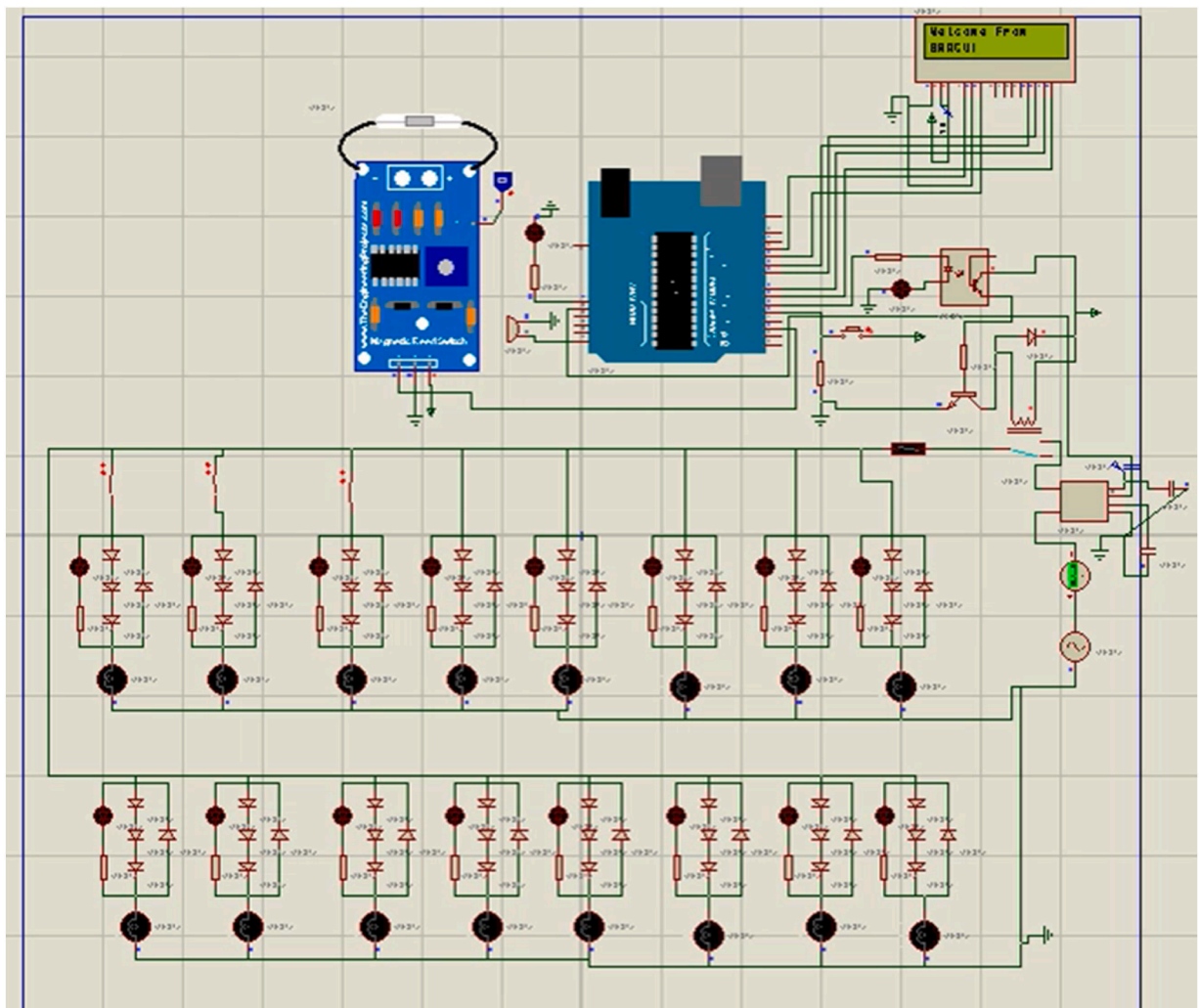


**Fig. 2.** A primary control circuit schematic. The Proteus schematic and simulation confirms the status of 16 LED on/off state. The LCD and CB were used for notification and safety purposes.

relay was used as a precautionary measure for the 220 V AC line to protect the small controller circuits.

Along with these, a few more safety measures were taken around the high-intensity ultraviolet lights such as using suitable eye protection and minimizing human exposure were essential. Ozone is formed as a byproduct of UV-C which is considered a health hazard to the operator. Ozone gas accumulates in closed cabinet designs and gets trapped during the decontamination procedure. Therefore, care has been taken to use low-pressure mercury lamps which emit a very small amount of ozone which is not considered harmful to the surrounding environment.

### 3.2. Control mechanism design

The UVC decontamination chamber has a door lock system while the disinfection process is going on, however, we cannot avoid the risk of health issues as the system will be manually operated. If any person opens the door while the machine is running, it can cause severe burns of the skin and eye injuries (photokeratitis). To solve this problem, we have designed a control circuit where the machine will operate automatically and safely. Moreover, the operator may be able to control and investigate the machine operation by using a control system unit.

The whole system will be controlled by an Arduino microcontroller. To do this we have proposed using an Arduino Uno microcontroller board based on the ATmega328P. UVC lamps will be controlled by a microcontroller with the help of a 5 V relay. For detecting door position whether it is closed, or not properly magnetic reed sensor is used. If anyone opens the door and tries to start the machine, he won't be able to do that. Similarly, if anyone opens the door while the machine is running, the machine will immediately stop working and show the message to the operator. To investigate internal temperature and humidity a DHT22 sensor is also used. These two sensors will send data to the microcontroller to control the machine. Three push switches are added to operate the machine properly. One switch will start the machine for the disinfection process while the door is closed for 5 min. Another push switch will show the sensor reading that the machine is running properly without any fault and the third push switch will help to reset the machine immediately.

For showing the output, a  $16 \times 2$  LCD (Liquid Crystal Display) screen is used where the user will be able to show if the door is properly closed or not, the remaining time of germ disinfection, sensor reading, etc. Two LEDs are attached, one is green, and another is red with the machine. The red LED indicated machine is powered up and ready to start and the green LED indicated purification process is going on. A buzzer is also attached to the microcontroller to give a signal when any interruptions occur, and the purification process is completed successfully.

The control circuit can be powered up through a microcontroller dc jack where we can give input in a range of 7 V–12 V. We can also power up by using 220 V AC to 12 V AC step down transformer as the circuit has a rectifier and voltage regulator attached.

While controlling the machine with a microcontroller there is less chance of knowing that every light is working properly. To solve these LED array indicators are designed to indicate whether each light is working or not. Each LED light indicated each UVC lamp is on or off. For example, LED one is on means first UVC lamp is on, third LED is off means third UVC lamp inside the machine is off which means it is damaged or disconnected. Each UVC lamp indicator circuit is built with combinations of four diodes, and one LED. For sixteen lamps it creates an array of this circuit with parallel connection. This circuit even works when inrush current or extra load current flows through the circuit because it detects load by using low voltage drop due to diodes instead of detecting load current. A primary circuit schematic is shown in Fig. 2.

Additionally, we have designed a control mechanism (Figs. 2 and 3) for automatic on/off the chamber and to identify the faulty LED light. We have also included an automatic timer to record the disinfection cycle time, temperature, and humidity (Fig. 3). We measured the irradiance of LED light and found the total intensity of  $10.32 \text{ mW/cm}^2$  and UV intensity  $1.55 \text{ J/cm}^2$  for lamp spacing 23 cm which is in good agreement with Stanford and other research groups findings. The similar dosage of fluence level is found to be most effective to kill the SARS-CoV-2 viruses. The final prototype has been shown in Fig. 4.

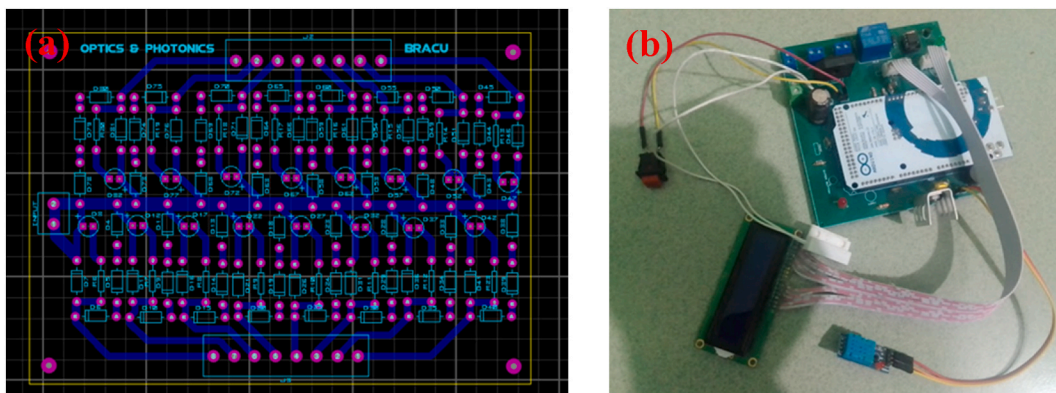


Fig. 3. PCB design of control mechanism (a) and hardware of the control mechanism (b).

### 3.3. Study design

The study of measuring the disinfection capacity of the UV-C chamber was designed by observing the viral load reduction and bacterial biochemical assay. At the inception of the study, the *Geobacillus* spore strip culture assay was conducted to validate the UV-C illumination chamber. The samples were divided into two groups, the control, and the test group. Samples in the control group underwent viral load determination and bacterial biochemical assay without getting exposed to UV type C radiation. As in the test group, the samples were exposed to UV type C radiation before the mentioned assays.

### 3.4. Sampling

A total of 42 masks were collected from patients with COVID-19 symptoms across Dhaka city with their full consent. Proper safety protocol was maintained during the sampling process. The masks were placed in zip-locked bags and carried in ice-contained iceboxes. Later, they were stored in the freezer (4 °C).

### 3.5. Inclusion criteria

We used three layered surgical masks from confirmed COVID-19 positive patients as our sample. The masks of doctors and health workers were the priority for the inclusion of the samples. Moreover, to ensure that the masks were used for a sufficient amount of time, we selected masks that were used for at least 24 h by the patients who were COVID-19 positive at the time of collection. Upon evaluating the mask samples on the inclusion criteria, the number of masks used in this study was five (n = 5).

### 3.6. Exclusion criteria

Masks that are made of cotton or other washable material rather than disposable three-layered surgical masks were not collected. KN95 masks were considered as an exclusion criterion as Bangladeshi people generally do not use KN95 masks extensively as surgical masks. Also, the masks were not taken from the patients who recovered from COVID-19 or had been stored for a very long time.

### 3.7. Sampling process

The collected masks were marked and cut into two 1 cm × 1 cm pieces. For the control group, one piece was added to the Viral Transport Medium (VTM). Then the VTM was vortexed to thoroughly mix with the portion of the mask before being stored in a –80 °C refrigerator for RNA extraction. Another piece was added to the TSB medium for further serial dilution and biochemical assay. As for the test group, a similar sampling process was performed after UV-C exposure.

### 3.8. UV-C illumination chamber validation analysis

*Geobacillus* spore strip culture assay was performed to validate the decontamination capacity of the UV-C Illumination Chamber. Commercially available *Geobacillus* spore strips were used as the sample in the validation assay (Supplementary Fig. S1).

### 3.9. Spore strips exposure

Six commercially available spore strips were used in this experiment and divided into two groups. For each group, two strips were exposed to UV-C radiation (Test), and one was not exposed to UV-C radiation (Control). Inside the UV-C cabinet, one strip adhered to the top rod, and another one was to the bottom rod using transparent tape. The strips were properly labeled beforehand. The exposure was done in 5 min. With care and precaution, both strips were detached from the rods.

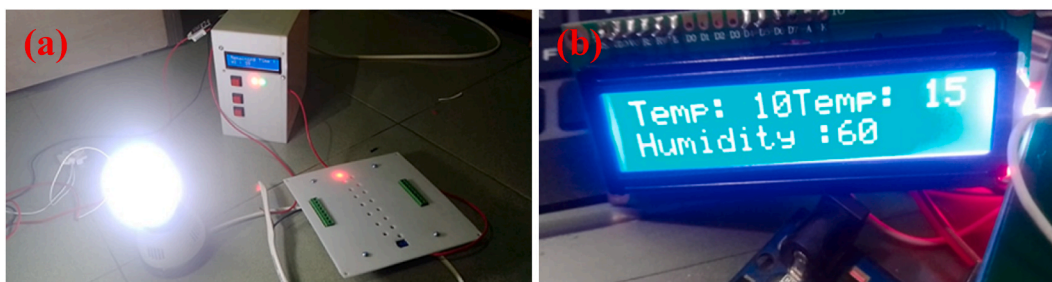


**Fig. 4.** Safety Box at left (a) which includes on/off switch and LED status indicator in right magnified (b) which shows the temperature and humidity inside UV-C chamber.

### 3.10. Inoculum preparation

Three TSB media tubes were collected for the inoculum preparation. The media tubes were properly labeled. Inside the laminar airflow hood, one intact sample spore strip and two post-UV-C exposed spore strips were transferred to the respectively labeled TSB media tubes with the help of sterilized tweezers. The inoculum preparation was completed, and the tubes were transferred into the incubator for bacterial growth. For both the groups, the incubation temperature was set to be at 52 °C. Group one and group two had seven and ten days of incubation period respectively.

### 3.11. Measurement of viral load

The viral load measurement was done by identifying the COVID-19 specific N-gene and ORF1 gene. RT-qPCR was used to detect and quantify them. A conclusive workflow was constructed for sample collection and RT-qPCR amplification (Fig. 5).

### 3.12. RNA extraction procedure

FavorPrep™ Viral DNA/RNA Kit (FAVORGEN Biotech Corporation, Taiwan) was used to extract the RNA and the protocol provided by the company was followed to run the experiment. The sample in VTM was vortexed and centrifuged to mix, and then the 140 µL sample was transferred to a tube with a micropipette. Then 560 µL of VNE and carrier RNA was added, vortexed, and kept for 10 min of incubation at room temperature. 560 µL ethanol was added to the sample and vortexed to mix. The kit collection tube had a VNE column attached. 700 µL of the sample mixture was then pipetted into the VNE column and centrifuged at 8000 RPM. The liquid was discarded, and the collection tube was reattached to the VNE column. This process was followed again for the rest of the samples. Ethanol-containing wash buffer 1 was put into the VNE column in a quantity of 500 µL and centrifugation was done at 8000 RPM, discarding the residual liquid. The VNE column was reattached to the collection tube. Ethanol-containing wash buffer 2 was put into the VNE column in a quantity of 650 µL and then centrifugation was done at 8000 RPM, discarding the residual liquid. The VNE column was reattached to the collection tube. Repeated this step. The VNE column was centrifuged at 18,000 RPM to dry it, and the remaining liquid and collection tube were discarded. 40 µL of RNase-free water was lastly added to the VNE column. The drop was placed in the VNE membranes center for better absorption. Then the VNE column was centrifuged at 18,000 RPM to elute RNA.

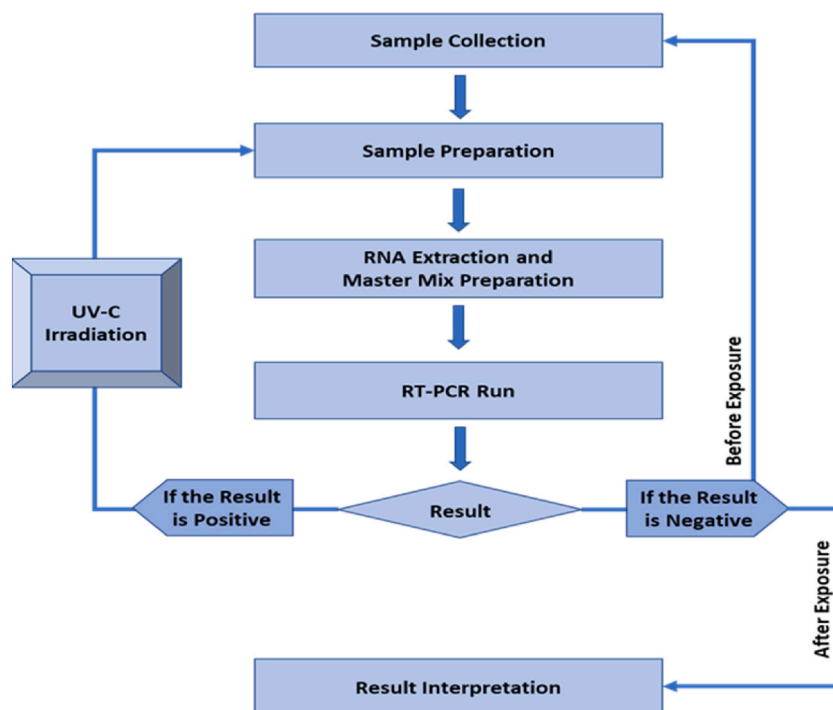


**Fig. 5.** Flowchart of sample collection and subsequent RT-qPCR amplification. The workflow starts with sample collection then sample preparation. Sample preparation is followed by RNA extraction and master mix preparation. After that RT-qPCR amplification was done and upon the observed result, mask sample with positive result underwent UV-C irradiation. The irradiation process is followed by sample preparation to result interpretation.

### 3.13. Master mix preparation and RT-qPCR amplification

The master mix was prepared by adding 4  $\mu\text{L}$  of a 2019-nCoV-PCR-Enzyme Mix (S3102E SC2 – Novel Coronavirus (2019-nCoV) Nucleic Acid Diagnostic Kit, Sansure Biotech Inc., China) with a 26  $\mu\text{L}$  of 2019-nCoV-PCR Mix in a PCR tube at room temperature. The same preparation was made for the positive and negative controls, which were necessary for the RT-qPCR run. Then the mixture was pipetted 5–6 times and needed to vortex for 1 min. After that, the mixture needed to spin for 5 s in a centrifuge machine. Then 10  $\mu\text{L}$  sample release reagent was added to the testing PCR tube and 10  $\mu\text{L}$  negative control to the negative control tube. The caps need to be closed tightly in the tube and spun for 5 s again. Lastly, 10  $\mu\text{L}$  of positive control was added to the PCR tube separately in the sample extraction room to prevent contamination of other sample PCR tubes.

### 3.14. Biochemical assay

The biochemical assay was conducted on the control and test group to identify the presence of different types of bacteria, and fungi. This characterization test is done frequently in various studies to identify and assess bacterial growth. Nowadays modern kits are also available to make those biochemical tests easier [39].

In this analysis, one mask sample was used. Both the control and test groups were diluted (1:1000) and vortex accordingly before lawn culture. After culturing, plates were kept in the incubator for 24 h at 37 °C. After the incubation period, the bacterial growth was checked, and verified the presence of different types of bacteria (Supplementary Fig. 2).

## 4. Results

### 4.1. Irradiance and dosage measurement

The UV sensor is placed at a different position of the chamber (Fig. 6) and the UV lights were removed gradually by 2. The data is then collected using Arduino and the above graph depicts the intensity at different points which are in the bottom left, upper right and middle of the chamber and the irradiance was measured (Fig. 6). When all 16 lights were active, the intensity was around 10  $\text{mW}/\text{cm}^2$ . The result stays similar up to 8 lights removed. At center position UV intensity is around 5.2  $\text{mW}/\text{cm}^2$  and dosage was 1.55  $\text{J}/\text{cm}^2$  in 180 s for lamp spacing 23 cm/9.05 inch (Fig. 7). The dosage limit is around 100  $\text{J}/\text{cm}^2$  up to which mask can perform better is around 100  $\text{J}/\text{cm}^2$ . The intensity starts to fall and when 2 lights are left (14 lights removed), the intensity found to be around 6  $\text{mW}/\text{cm}^2$ . After the 180s the intensity became saturated.

Fig. 7 shows the irradiance with respect to UVC light activation/deactivation status. The dosage can be calculated as dose = irradiance\*time (Fig. 7). The maximum UV intensity is around 1.55  $\text{J}/\text{cm}^2$  till 8 Rem (8 lights removed) and then irradiance falls significantly. The dosage is shown to be 1.55  $\text{J}/\text{cm}^2$  in 180 s for lamp spacing 23cm/9.05 inch. Fig. 7 b shows the same result as Fig. 7 a except the light intensity is shown in  $\text{mW}/\text{cm}^2$  instead of  $\text{J}/\text{cm}^2$ .

### 4.2. Geobacillus spore strip culture

After the incubation period, the positive inoculum showed up yellow in hue, whereas the inoculums from the two test samples looked transparently purple (Fig. 8).

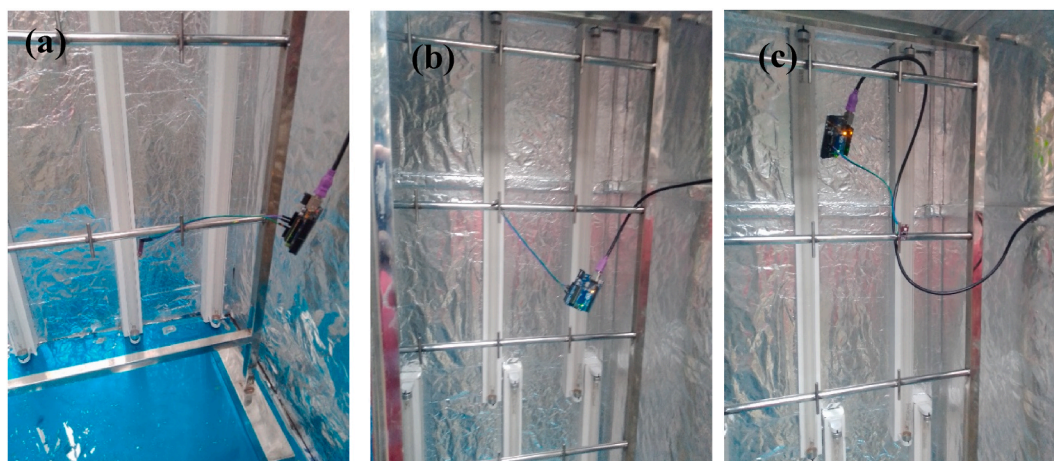


Fig. 6. Placing GUVVA-S12SD model UV sensor at different location: (a) bottom. (b) Middle and (c) right.



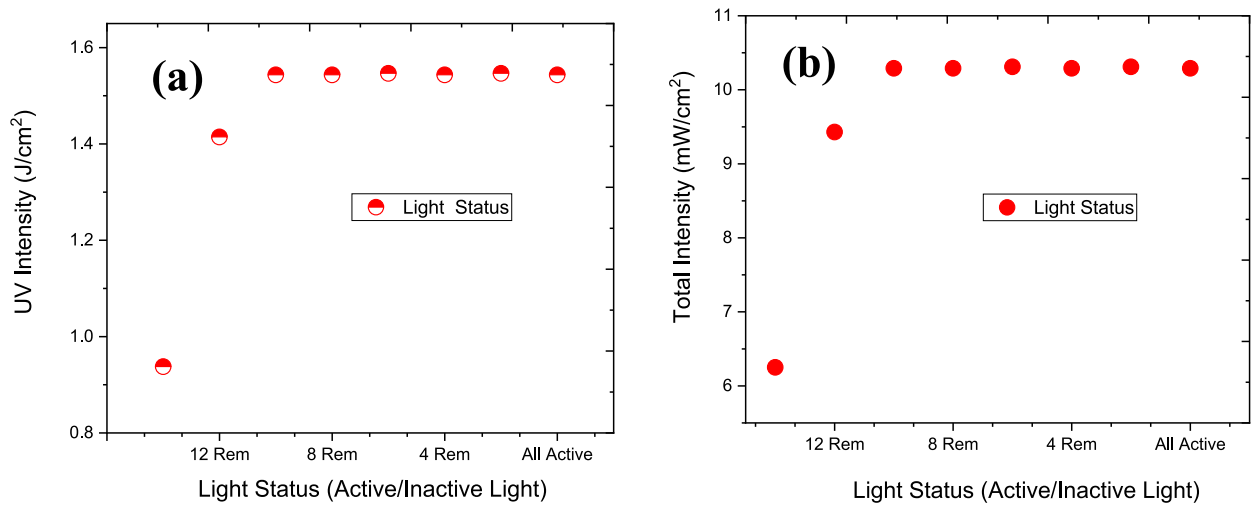


Fig. 7. UV and total intensity due to activation and deactivation of UVC light.

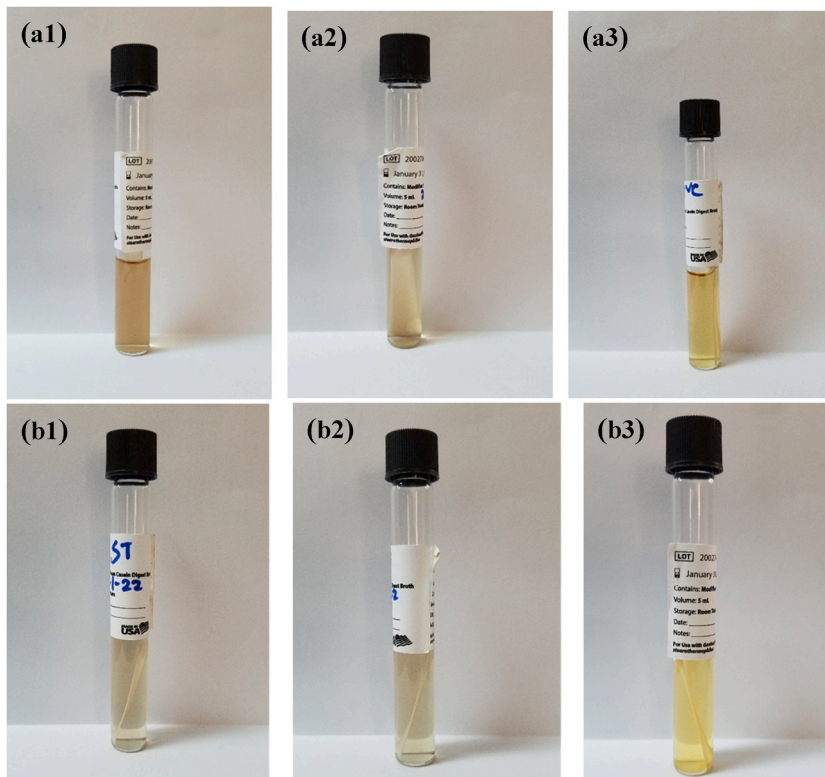


Fig. 8. The *Geobacillus* spore strips were incubated, and media was observed. Group 1 (3 strips) was incubated for 10 days at 50 °C and group 2 (3 strips) was incubated for 7 days at 50 °C. The *Geobacillus* spore strips used in a.1, a.2, b.1, and b.2 underwent UV type C irradiation. After incubation, showed a transparent purple color indicating no bacterial growth. The *Geobacillus* spore strips used in a.3 and b.3 as control were not exposed to UV type C irradiation. Thus, showed a yellow color indicating the presence of bacterial growth. (For interpretation of the references to color in this figure legend, the reader is referred to the Web version of this article.)

#### 4.3. Viral load determination

We assessed the RT-qPCR results to compare differences between before and after UV-C exposed samples. In this study, N gene and ORF1ab protein are used as the target for RT-qPCR to detect them as COVID-19 positive. The COVID-19 causing genes are the N gene and ORF1ab proteins. In COVID-19 genome, ORF1ab consists of two-thirds of the 5' genome whereas, surface protein (S), envelope

protein (E), membrane protein (M), and nucleocapsid protein (N) is in one-third of 3' genome [40] (Table-1; Fig. 9). The N gene is primarily responsible, and the outcome is mostly determined by its CT value [35,41,42].

#### 4.4. Biochemical assay

Out of seven agar media, five agar media showed bacterial growth. The bacterial growth implies the presence of *Staphylococcus aureus*, Methicillin-resistant *Staphylococcus aureus*, Group B streptococci strain, *Staphylococcus aureus*, and Gram-negative enteric bacteria. On the other hand, Pseudomonas agar base and Chromatic Candida agar did not show any growth meaning the absence of *Pseudomonas aeruginosa* and Candida respectively (Table 2; Supplementary Fig. 3).

## 5. Discussion

The purpose of observing the culture of commercially available *Geobacillus* spore strips was to validate the disinfection capacity of the UV-C illumination chamber. Because of the pH change brought on by bacterial growth, the positive inoculum's color changes to yellow, acting as a chemical indicator. Dextrose from TSB is used by microorganisms to make acid as a byproduct, which changes its color to yellow to signify bacterial growth [43]. The test sample inoculums, on the other hand, had a clear purple appearance and no signs of bacterial growth. With this, we can see that the UV-C chamber's construction and validation are both valid.

This unprecedented global pandemic caused by the COVID-19 virus has shaken the healthcare system to recognize the importance of sterile personal protective equipment (PPE). The information from the current study is comparable to the earlier published data. According to some studies, the UV-C decontamination system removes almost all viruses from the surfaces of filtering facepiece respirators (N95 masks) [3,44–46]. Our study aims to appreciate the reusability of personal protective equipment and proper disposal of it. The use of UV type C radiation has proven to be effective in viral and bacterial load reduction. There was also the talk of using heat and alcohol-based sprays to sterilize and reuse face masks in order to cope with the expense and availability of face masks during the COVID-19 pandemic [47].

Based on the findings, the genes responsible for COVID-19 such as N, and ORF1ab are no longer found in the after-exposed mask samples. The result is considered accurate because both groups showed a standard result which means the reagents worked properly and no contamination occurred during the test. It indicates that the UV-C light used in the chamber possesses the ability to eradicate the COVID-19 virus and the duration of exposure time is also enough. The RT-qPCR was set in four stages, 50 °C for 30 min, 1 cycle in stage 1. Stage 1 is followed by stage 2 of one cycle for 1 min at 95 °C. After stage 2, for 15 s and 31 s a total of 45 cycles were run at 95 °C and 60 °C respectively in stage 3. Following the 3rd stage, the process was run for one cycle in 25 °C for 10 s in stage 4. In this study the RT-qPCR was selective for N gene, ORF1ab gene and internal control.

This study also has a few limitations. Firstly, detecting COVID-19 responsible genes from the collected mask samples was not conducted on the day of mask collection. It enhanced the chance of missing a particular gene in the RT-qPCR analysis. Furthermore, the sample size was inadequate for the experiment. Due to resource constraints, only surgical face masks were used in this experiment, rather than other types of PPE.

In Table-2 it shows that the sample did not contain candida. The absence of candida indicates there is no potential fungal infection. However, other culture plates provided us with information that the sample contained mentioned micro-organisms in the control group. The observed microorganisms were not found in the test group which indicated that the UV-C radiation acted as bactericidal and killed the bacteria.

Therefore, it seemed that the decontamination method using the UV-C chamber would be quite easier for some target health service sectors. Lastly, continuous monitoring and research are still required to improve this chamber's performance.

## 6. Conclusion

To conclude, in this study, we constructed an automated low-cost UV-C chamber with locally available materials for facepiece, PPE, pathogen and other biological sample decontamination purposes. To confirm the efficacy of the device we performed the *Geobacillus* spore strip culture assay, viral load measurement, RT-qPCR measurement, and biochemical assay on different types of bacteria, and fungi. We observed viral genetic material can be effectively reduced by this disinfection tool in the mask samples. Also bacterial colonies have been observed to be significantly less in the mask samples that underwent UV-C irradiation. Additionally, the

**Table 1**

CT values (cycle) determined from RT-qPCR results. The values are of IC, N gene and ORF1ab gene. Before UV-C: Control Group. After UV-C: Test Group.

Sample	IC (Before UV-C)	IC (After UV-C)	N (Before UV-C)	N (After UV-C)	ORF1ab (Before UV-C)	ORF1ab (After UV-C)
Sample 1	15.44	0	11.69	0	9.84	0
Sample 2	11.54	0	12.31	0	6.74	0
Sample 3	10.95	0	0	0	5.18	0
Sample 4	11.17	3.69	13.56	0	12.78	0
Sample 5	14.66	10.56	8.19	0	0	0
Average	12.752	2.85	9.15	0	6.908	0

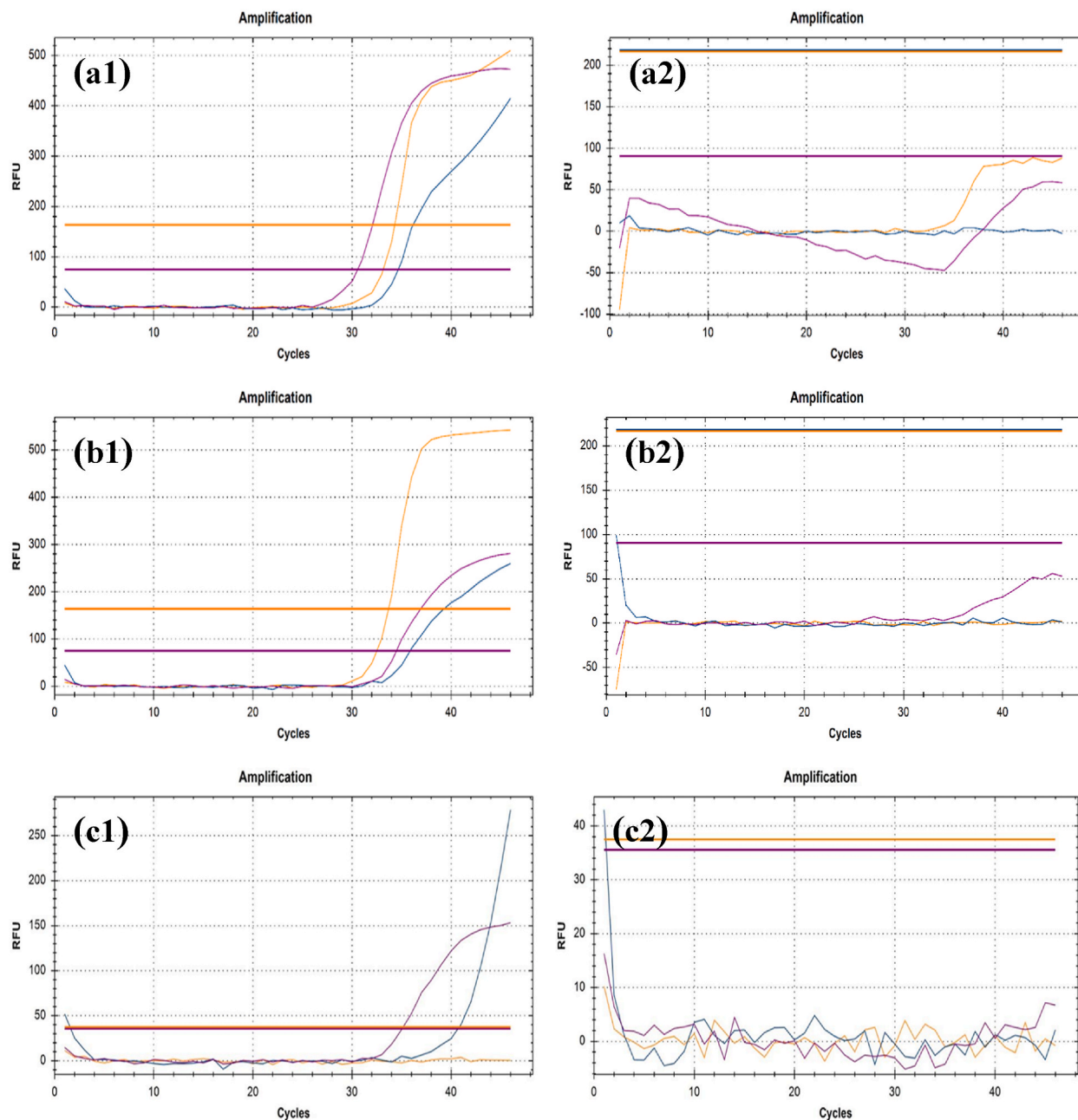


**Fig. 9.** Viral load is represented as amplification graphs of RT-qPCR. Internal Control (IC) gene, N gene and ORF1ab gene are shown in purple, yellow, and blue color respectively in the graphs. The RT-qPCR results of mask samples before the UV-C exposure are shown in a.1, b.1, c.1, d.1 and c.1. On the other hand, the results of UV-C exposed mask samples are projected in a.2, b.2, c.2, d.2 and e.2. The presence of the N gene is observable in a.1, b.1, c.1, d.1 and c.1. ORF1ab gene can be seen in a.1, b.1, c.1 and d.1. Internal Control gene is observable in a.1, b.1, d.1 and e.1. The ORF1ab and IC gene are nonexistent in a.2, b.2, c.2, d.2 and e.2. Also, the N gene cannot be found in a.2, b.2, c.2 and d.2. All the related CT values can be found in [Table 1](#). (For interpretation of the references to color in this figure legend, the reader is referred to the Web version of this article.)

biochemical assay confirms the presence of different types of bacteria, and fungi before and after UVC exposure. To conclude, we can safely say that our UV-C illumination chamber has the potential to be used in healthcare settings. This technology holds high potential in reusability of personal protective equipment. Only surgical face masks were used in this study. We will be observing the decontamination potential on other PPE. This method of disinfection will be beneficial for both economical perspective and environmental safety.

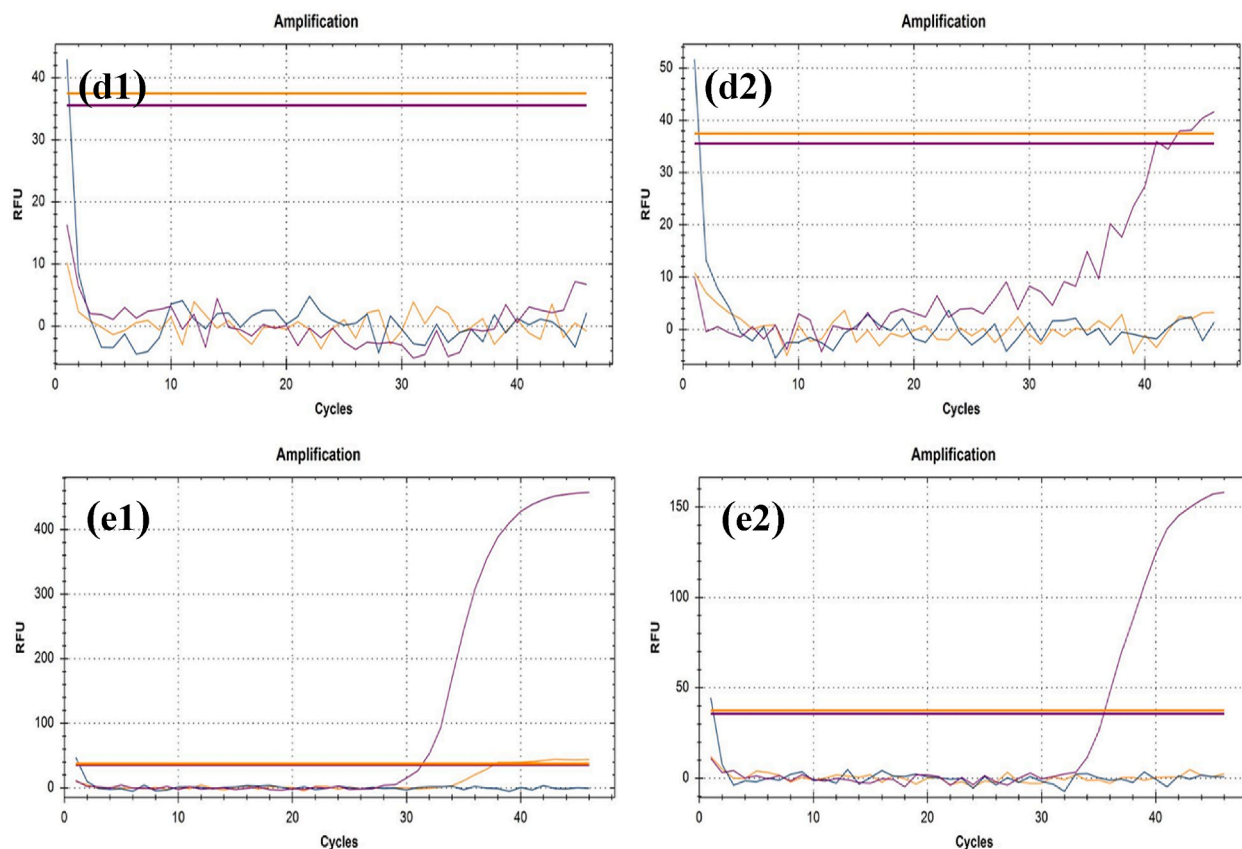


Fig. 9. (continued).

Table-2

Biochemical assay to determine the presence of different types of microorganism in the control and test group.

Sl.	Agar Media	Organism	Growth Control Group (Before UV-C Exposure)	Growth Test Group (After UV-C Exposure)
1	Chromatic Staph Aureus culture media	<i>Staphylococcus aureus</i>	Yes	No
2	Chromatic MRSA Agar Base	Methicillin-resistant <i>Staphylococcus aureus</i>	Yes	No
3	Chromatic Strepto B	Group B streptococci strain	Yes	No
4	Mannitol Salt Agar	Pathogenic Staphylococci	Yes	No
5	MAC CONKEY	Gram-negative enteric bacteria	Yes	No
6	Pseudomonas Agar base	<i>Pseudomonas aeruginosa</i>	Yes	No
7	Chromatic Candida	Candida	No	No

### Data availability statement

The data that support the findings of this study are available from the corresponding author upon reasonable request.

### Declaration of competing interest

The authors declare that they have no known competing financial interests or personal relationships that could have appeared to influence the work reported in this paper.

### Acknowledgement

We would like to acknowledge Brac University and Optica (formerly OSA) for financial support and Stanford University, USA for technical support. Additionally, we would like to acknowledge Ashley Rene Styczynski from Stanford University, USA for the

*Geobacillus stearothermophilus* Spore's Samples and GUV C T21GH UV sensor module. We would like to thank Anirudha, Al-Amin, Ahmed, Rajib, Monica, Sara, and Maisha for their support.

## Appendix A. Supplementary data

Supplementary data to this article can be found online at <https://doi.org/10.1016/j.heliyon.2024.e26348>.

## References

- [1] G. Ibanez-Cervantes, et al., Disinfection of N95 masks artificially contaminated with SARS-CoV-2 and ESKAPE bacteria using hydrogen peroxide plasma: impact on the reutilization of disposable devices, *Am. J. Infect. Control* 48 (9) (Sep 2020) 1037–1041.
- [2] K O H e al, Ultraviolet germicidal irradiation of filtering facepiece respirators: a systematic review, *J. Hosp. Infect.* 106 (2) (2020) 163–175.
- [3] M. Puschke, et al., Construction and validation of UV-C decontamination cabinets for filtering facepiece respirators, *Appl. Opt.* 59 (25) (2020) 7585–7595, 09/01/2020.
- [4] A. Kumar, et al., Decontamination of N95 masks for re-use employing 7 widely available sterilization methods, *PLoS One* 15 (12) (2020) e0243965.
- [5] J.W. Limei Hao, Enlei Zhang, Ying Yi, Zongxing Zhang, Jinming Zhang, Jiancheng Qi, Disinfection efficiency of positive pressure respiratory protective hood using fumigation sterilization cabinet, *Biosafety and Health* 1 (1) (2019) 46–53.
- [6] D.U.- AY Starikovskiy, Medical Mask with Plasma Sterilizing Layer, arXiv preprint arXiv:2004.00807, 2020.
- [7] F.A. Carrillo IO, C.M. Valverde, T.N. Tingle, F.R. Zabaneh, Immediate-use steam sterilization sterilizes N95 masks without mask damage, *Infect. Control Hosp. Epidemiol.* 41 (9) (2020 Sep) 1104–1105.
- [8] M. Stibich, J. Stachowiak, B. Tanner, M. Berkheiser, L. Moore, I. Raad, R. Chemaly, Evaluation of a pulsed-xenon ultraviolet room disinfection device for impact on hospital operations and microbial reduction, *Infect. Control Hosp. Epidemiol.* 32 (3) (2011) 286–288.
- [9] M. R. B.M. Andersen, K. Hochlin, F.-H. Jensen, P. Wismar, J.-E. Fredriksen "Decontamination of rooms, medical equipment and ambulances using an aerosol of hydrogen peroxide disinfectant" *J. Hosp. Infect.*, vol. 62, no. 2, pp. 149–155.
- [10] E.D.F. Scaglione, G. Mantova, V. Caturano, A. Stornaiuolo, A. D'Anna, P. Salvatore, An experimental analysis of five household equipment-based methods for decontamination and reuse of surgical masks, *Int. J. Environ. Res. Publ. Health* 19 (19) (2022) 3296.
- [11] D. Poppendieck, Tool for evaluation of vaporized hydrogen peroxide disinfection of N95 masks in small rooms [online], in: Technical Note (NIST TN), National Institute of Standards and Technology, Gaithersburg, MD, 2020.
- [12] W. Ahmed, C.W. Lim, Effective recycling of disposable medical face masks for sustainable green concrete via a new fiber hybridization technique, *Construct. Build. Mater.* 344 (2022) 128245, 08/15/2022.
- [13] B. Atilgan Türkmen, Life cycle environmental impacts of disposable medical masks, *Environ. Sci. Pollut. Control Ser.* 29 (17) (2022) 25496–25506, 04/01/2022.
- [14] R. Rathinamoorthy, S. Raja Balasaraswathi, Mitigation of microfibers release from disposable masks – an analysis of structural properties (in en), *Environ. Res.* 214 (2022) 114106, 11/01/2022.
- [15] R. Yan, S. Chillrud, D.L. Magadini, B. Yan, Developing home-disinfection and filtration efficiency improvement methods for N95 respirators and surgical facial masks: stretching supplies and better protection during the ongoing COVID-19 Pandemic, *J. Int. Soc. Respir. Prote.* 37 (1) (2020 2020) 19–35.
- [16] P. Morganti, G. Morganti, Surgical & beauty facial masks- the new waste problem of post COVID-19, *Biomed. J. Sci. Tech. Res.* 29 (5) (2020) 22945–22950.
- [17] M. Muhyuddin, et al., Waste face surgical mask transformation into crude oil and nanostructured electrocatalysts for fuel cells and electrolyzers, *ChemSusChem* 15 (2021), 12/01/2021.
- [18] F. Torres, G. De-la-Torre, Face mask waste generation and management during the COVID-19 pandemic: an overview and the Peruvian case, *Sci. Total Environ.* 786 (2021) 147628, 05/01/2021.
- [19] N. Ferronato, V. Torretta, Waste mismanagement in developing countries: a review of global issues, *Int. J. Environ. Res. Publ. Health* 16 (6) (2019) 1060, 01//2019.
- [20] C. Nzediegwu, S. Chang, Improper solid waste management increases potential for COVID-19 spread in developing countries, *Resour. Conserv. Recycl.* 161 (2020) 104947, 05/01/2020.
- [21] T.A. Aragaw, Surgical face masks as a potential source for microplastic pollution in the COVID-19 scenario, *Mar. Pollut. Bull.* 159 (2020) 111517, 10/25/2020.
- [22] J. Delgado-Gallardo, et al., Disposable FFP2 and type IIR medical-grade face masks: an exhaustive analysis into the leaching of micro- and nanoparticles and chemical pollutants linked to the COVID-19 pandemic, *ACS ES&T Water* 2 (4) (2022) 527–538, 04/08/2022.
- [23] A. Jemec Kokalj, et al., Environmental hazard of polypropylene microplastics from disposable medical masks: acute toxicity towards *Daphnia magna* and current knowledge on other polypropylene microplastics, *Microplast. Nanoplast.* 2 (1) (2022) 1, 01/04/2022.
- [24] M.P.G. Mol, S. Caldas, Can the human coronavirus epidemic also spread through solid waste? *Waste Manag. Res.* 38 (5) (2020) 485–486, 05//2020.
- [25] F. Shiferie, Improper disposal of face masks during COVID-19: unheeded public health threat, *Pan Afr. Med. J.* 38 (2021) 366.
- [26] M. Raeiszadeh, B. Adeli, A critical review on ultraviolet disinfection systems against COVID-19 outbreak: applicability, validation, and safety considerations, *ACS Photonics* 7 (2020), 10/14/2020.
- [27] I. Teo, et al., Healthcare worker stress, anxiety and burnout during the COVID-19 pandemic in Singapore: A 6-month multi-centre prospective study (in en), *PLoS One* 16 (10) (2021) e0258866, 10/22/2021.
- [28] B. van Straten, et al., A life cycle assessment of reprocessing face masks during the COVID-19 pandemic, *Sci. Rep.* 11 (1) (2021) 17680, 09/03/2021.
- [29] J. Howard, et al., An evidence review of face masks against COVID-19, *Proc. Natl. Acad. Sci. U. S. A.* 118 (4) (2021) e2014564118, 01/26/2021.
- [30] J. Chakma, 25 lakh masks sold daily, in: *The Daily Star*, News Portal, 2021, 08/01/T00:00:00+06:00 2021.
- [31] [Oecd.org](https://oecd.org), The Face Mask Global Value Chain in the COVID-19 Outbreak Evidence and Policy Lessons - OECD, OECD, 2020, 05/04/2020.
- [32] [NobelPrize.org](https://nobelprize.org), The Nobel prize in physiology or medicine 1903, (in en-US), [NobelPrize.org](https://nobelprize.org).
- [33] C.S. Heilingloh, et al., Susceptibility of SARS-CoV-2 to UV irradiation (in en), *Am. J. Infect. Control* 48 (10) (2020) 1273–1275, 10/01/2020.
- [34] S. K. Moore, "Ultraviolet-LED Maker Demonstrates 30-Second Coronavirus Kill - IEEE Spectrum," (in en), [IEEE Spectrum](https://www.ierspectrum.com).
- [35] L.R. Dougall, J.B. Gillespie, M. Maclean, I.V. Timoshkin, M.P. Wilson, S.J. MacGregor, Pulsed ultraviolet light decontamination of artificially-generated microbiological aerosols, in: 2017 IEEE 21st International Conference on Pulsed Power (PPC), 2017, pp. 1–5.
- [36] S. Mechler, COVID-19 pandemic: disinfection and sterilization of face masks for viruses (in en-US), in: *Consolidated Sterilizer Systems*, 2020, 03/18/T13:10:44+00:00 2020.
- [37] L. Kalter, Coronavirus Puts UV in the Disinfectant Spotlight, [WebMD](https://www.webmd.com), 2020.
- [38] J.P. Wilde, T.M. Baer, L. Hesselink, Modeling UV-C irradiation chambers for mask decontamination using Zemax OpticStudio, *Appl. Opt.* 59 (25) (2020) 7596–7605, 09/01/2020.
- [39] T. Hussain, et al., Biochemical characterization and identification of bacterial strains isolated from drinking water sources of Kohat, Pakistan, *Afr. J. Microbiol. Res.* 7 (16) (2013) 1579–1590.
- [40] R.A. Khailany, M. Safdar, M. Ozaslan, Genomic characterization of a novel SARS-CoV-2 (in en), *Gene Reports* 19 (2020) 100682, 06//2020.
- [41] R.K. Gill, et al., Color-coding of microchip RT-PCR test system for SARS-CoV-2 detection, *J. Biosci. Med.* 9 (5) (2021) 94–119, 05/06/2021.

- [42] J.V. Waller, et al., Diagnostic tools for coronavirus disease (COVID-19): comparing CT and RT-PCR viral nucleic acid testing, *Am. J. Roentgenol.* 215 (4) (2020) 834–838, 10//2020.
- [43] H. Albert, D.J.G. Davies, L.P. Woodson, C.J. Soper, "Biological indicators for steam sterilization: characterization of a rapid biological indicator utilizing *Bacillus stearothermophilus* spore-associated alpha-glucosidase enzyme," (in en), *J. Appl. Microbiol.* 85 (5) (1998) 865–874.
- [44] M. Bentancor, et al., LUCIA: an open-source device for disinfection of N95 masks using UV-C radiation (in eng), *HardwareX* 9 (2021) e00181, 04//2021.
- [45] B.J. Kayani, et al., UV-C tower for point-of-care decontamination of filtering facepiece respirators (in eng), *Am. J. Infect. Control* 49 (4) (2021) 424–429, 04//2021.
- [46] K. Seresirikachorn, et al., Decontamination and reuse of surgical masks and N95 filtering facepiece respirators during the COVID-19 pandemic: a systematic review, *Infect. Control Hosp. Epidemiol.* 42 (1) (2021) 25–30, 01//2021.
- [47] M.C. Celina, et al., Extended use of face masks during the COVID-19 pandemic - thermal conditioning and spray-on surface disinfection (in eng), *Polym. Degrad. Stabil.* 179 (2020) 109251, 09//2020.